ACS APPLIED MATERIALS & INTERFACES

Research Article

www.acsami.org

Micro-Pseudocapacitors with Electroactive Polymer Electrodes: Toward AC-Line Filtering Applications

Narendra Kurra,[+] Qiu Jiang,[+] Ahad Syed, Chuan Xia, and Husam N Alshareef*

Materials Science and Engineering, King Abdullah University of Science and Technology, Thuwal 23955-6900, Saudi Arabia

Supporting Information

ABSTRACT: In this study, we investigate the frequency response of micro-pseudocapacitors based on conducting polymer electrodes such as poly(3,4-ethylenedioxythiophene) (PEDOT), polypyrrole, and polyaniline. It is shown that by proper choice of polymeric material and device structure, miniaturized micro-pseudocapacitors can match the frequency response of commercial bulky electrolytic capacitors. Specifically, we show that PEDOT-based micro-pseudocapacitors exhibit phase angle of −80.5° at 120 Hz, which is comparable to commercial bulky electrolytic capacitors, but with an order of magnitude higher capacitance density (3 FV/cm^3). The tradeoff between the areal capacitance (C_A) and frequency response in the two-dimensional architecture (C_A = 0.15 mF/cm^2, phase angle of −80.5° at 120 Hz) is improved by designing three-dimensional thin-film architecture (C_A = 1.3 mF/cm^2, phase angle of −60° at 120 Hz). Our work demonstrates that fast frequency response can be achieved using electroactive polymer electrodes.

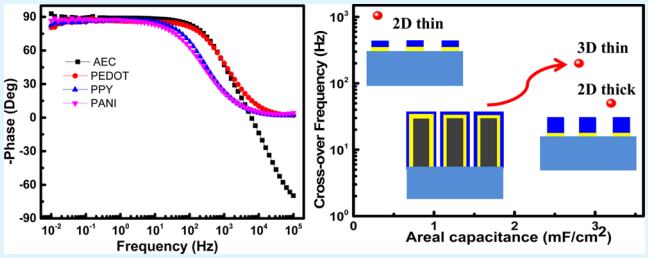

KEYWORDS: *ac-line filtering, conducting polymer, electrochemical capacitor, thin film, micro-pseudocapacitor*

Downloaded via KING ABDULLAH UNIV SCI TECHLGY on March 23, 2021 at 04:18:20 (UTC).
See https://pubs.acs.org/sharingguidelines for options on how to legitimately share published articles.

1. INTRODUCTION

Aluminum electrolytic capacitors (AECs) are currently being employed in alternating current (ac) line-filtering applications.[1−4] However, because of their bulky size and limited areal (or volumetric) capacitances, miniaturized electrochemical capacitors are under consideration to replace AECs.[5,6] Typically, for ac-line filtering, the capacitor must exhibit an impedance phase angle of at least −80° at a frequency of 120 Hz (ideal phase angle of −90° at 120 Hz).[1−6] Traditional supercapacitors, trade name for electrochemical double-layer capacitors, exhibit superior areal (or volumetric) capacitance over AECs, but are often characterized by a phase angle of 0° at 120 Hz.[7] This is because the internal and intricate porous structure of activated carbon electrodes limits the rate of ion diffusion, making electrochemical double-layer capacitors unfit for ac-line filtering.[1,2] However, other nanocarbon incarnations such as carbon nanotubes, graphene, and their derivatives have been explored for ac-line filtering applications due to their excellent electrical conductivity (10−300 S/cm) and fast ion diffusion kinetics.[1,5,6] Miller et al. have demonstrated vertically grown graphene (thickness, 600 nm) by chemical vapor deposition (CVD) on Ni as a suitable device for ac-line filtering.[1] Similarly, other open porous carbon nanostructures such as ultrathin films of carbon nanotube (CNT) and reduced graphene oxide have been demonstrated with good frequency response characteristics.[8−13] Recently, fast response supercapacitors based on graphitic ordered mesoporous carbons with voltage ratings up to 40 V were demonstrated.[12] Lim et al. have shown the ac-line filtering capability of crystalline graphene nanostructures carved by unzipping of CNTs.[13] Moreover, for compatible integration with other electronic components on a microchip (integrated circuit), electrochemical capacitors must be fabricated in planar format.[5] Thus, micro-electrochemical capacitor with planar diffusion of electrolyte ions could exhibit high power capabilities over conventional sandwich configuration.[14] Micropower sources with ac-line filtering capability are highly desirable for developing miniaturized electronic devices. Tour et al. have demonstrated three-dimensional (3D) graphene/CNT-based micro-electrochemical capacitors for ac-line filtering applications.[5] The key criterion lies in interplay between the electronic and ionic conductivity of electrochemical capacitor to achieve the desired frequency response.[1,5]

The common features of all these attempts are based on *non-Faradaic carbonaceous materials,* both in the thin film and 3D architectures *for demonstrating ac-line filtering applications. However, pseudocapacitive materials offer higher capacitance than carbon-based electrodes, and could therefore be a better option if their frequency response can match that of electrolytic capacitors. Indeed, it has been challenging to realize pseudocapacitive electrodes that match the electrolytic capacitors frequency response because kinetics of redox events tend to be limited by the rate of ion diffusion across conventional capacitor structure.*

Among pseudocapacitive materials, conducting polymers exhibit superior electrical conductivity over transition metal oxides/hydroxides, and are therefore promising materials to be investigated for high power applications.[15] In addition,

Received: December 30, 2015
Accepted: May 5, 2016
Published: May 5, 2016

 © 2016 American Chemical Society

DOI: 10.1021/acsami.5b12784
ACS Appl. Mater. Interfaces 2016, 8, 12748−12755

conducting polymer electrodes offer additional advantages over carbon-based materials in terms of ease and cost-effective solution processing at room temperature, unlike the high temperature growth processes and complex solution processing methods required for the latter. Thus, in this study, we systematically investigated the frequency response and pseudocapacitance of micro-pseudocapacitors (MPCs) based on conducting polymer electrodes with 2D and 3D current collector designs, including poly(3,4-ethylenedioxythiophene) (PEDOT), polypyrrole (PPY), and polyaniline (PANI). *Among the electroactive materials studied, we demonstrate that PEDOT micro-pseudocapacitors in two-dimensional (2D) architecture exhibit frequency response matching that of commercial electrolytic capacitors, while 3D architecture shows the potential for improving both frequency response and areal capacitance.*

2. EXPERIMENTAL SECTION

Materials. Chemicals were used as received without further purification. Analytical grade H_2SO_4 and 3,4-ethylenedioxythiophene (EDOT), aniline (ANI), pyrrole (PY), and surface active reagent sodium dodecyl sulfate (SDS, $CH_3(CH_2)_{11}OSO_3Na$) were purchased from Sigma-Aldrich.

Device Fabrication. *Two-Dimensional Interdigitated Thin Film Electrodes.* Glass substrates 1 × 1″ size (Fisher), cleaned with a soap solution to remove the dirt, followed by ultrasonication in acetone, isopropanol, and deionized (DI) water sequentially for 5 min each and then dried by blowing nitrogen. Photoresist ECI AZ3027 was spun coated at 3000 rpm for 30 s over the glass substrate to get 4 μm thick photoresist layer. Photoresist-coated substrates were soft baked at 100 °C for 1 min. The exposure was done using EVG contact aligner at a constant dose of 200 mJ/cm^2 through the Cr/glass mask having the patterns of interest. After the exposure, samples were developed in AZ726 developer solution for 1 min, which resulted in the formation of patterns on the photoresist layer. Metal layers of 250 nm Au/20 nm Ti were deposited by sputtering (Equipment Support Co, Cambridge, England) technique over the patterned photoresist layer. Lift-off was done using acetone followed by washing with DI water and dried by blowing N_2 gas. Geometric parameters of interdigitated fingers have a typical width of 100 μm and length of 5000 μm, while varied interspacings of 10−100 μm.

Three-Dimensional Interdigitated Silicon Electrodes. Si (100) (p-type, resistivity = 5 mΩ·cm) wafer (thickness, 525 μm) was *etch-through* employing photolithography and deep reactive ion etching (DRIE). DRIE is an effective process in fabricating 3D structures.[14,15] Initially, a Si substrate was coated with 10 μm thick photoresist (AZ9260) at 2400 rpm for 60s, followed by 180s soft baking at 110 °C. Then a Si wafer, which needs to be etched through, was bonded onto the photoresist-coated Si substrate. Further, the top Si wafer was coated again with the same photoresist followed by exposure through the etch mask at a constant dose of 1800 mJ/cm^2. The resist was develpoed using AZ726 developer to remove the exposed regions of the photoresist, and to gain access to the Si regions to be etched away by DRIE. The entire thickness of Si wafer was etch-through to obtain interdigitated 3D Si fingers.[16,17] DRIE was performed in an Oxford Instruments PlasmaLab100 at a temperature of −20 °C. Sequential SF_6 etching and C_4F_8 passivation steps are done with a time duration of 7 and 5 s, respectively. The passivation step deposits a hydrophobic fluoropolymer coating that protects against sidewall erosion as etching goes deeper into the silicon wafer.[16] The process conditions for the deposition cycle included a gas flow (C_4F_8/SF_6) of 100/5 sccm flowing at 30 mTorr, plasma power of 5 W, and coil power of 1300 W. Similarly, etch cycle plasma was generated by a power of 30 W and (C_4F_8/SF_6) gas flow of 5/100 sccm with the other process conditions similar to deposition cycle. The DRIE was done for a total of 1400 cycles to etch through the silicon and stop at the photoresist used for bonding with the bottom Si wafer. Further, the 3D interdigitated Si wall structures were metallized by sputtering 250 nm Au/20 nm Ti. Metal layers deposited over the photoresist present in the interspaces were removed by mild washing in acetone. This final step resulted in the formation of 3D Au/Si interdigitated wall structures.

Electrochemical Deposition of Conducting Polymers. Anodic polymerization of aqueous electrolytic monomeric baths was employed in electropolymerizing of PEDOT, PPY, and PANI films using standard three-electrode configuration in a glass cell.[18−20] Substrates consisting of Au/patterned photoresist/glass or Au/Si were used as working electrode, platinum wire as a counter electrode, and Ag/AgCl as a reference electrode at room temperature. PEDOT was electrochemically grown on Au surface employing an equimolar (10 mM) solution of EDOT and SDS (supporting electrolyte, 1 M H_2SO_4). Potentio-dynamic mode was used in which the potential was swept from 0 to 1.1 V at a scan rate of 100 mV/s (vs Ag/AgCl) for different number of cycles (CHI 660 D Electrochemical workstation). Electrolytic baths containing 0.1 M aniline and 1 M H_2SO_4 were used to electrodeposit PANI at a scan rate of 100 mV/s from −0.2 to 0.9 V versus Ag/AgCl.[21] The electrodeposition of PPY was performed potentiodynamically between the potential limits of 0 and 1 V versus Ag/AgCl at scan rate of 200 mV/s in an electrolytic bath containing 0.05 M pyrrole, 1 M H_2SO_4, and 0.0001 g/mL SDS. After the electrochemical deposition, the samples were thoroughly washed with DI water to remove any surfactant molecules adsorbed on the surface. Thickness of the deposited polymers was controlled through number of deposition cycles.

Material Characterization. Surface morphology and microstructure of the polymer films were imaged by scanning electron microscope (SEM; Nova Nano 630 instrument, FEI Co, The Netherlands). Atomic force microscopy (AFM) imaging (MFP-3D, Asylum Research) was done using Si probes (model, RTESPA, spring constant 40 N/m) in tapping mode. AFM 3D and roughness analysis was done using WSxM software 4.0 Beta 7.0.[22] The film thicknesses were measured using a Veeco Dektak 150 surface profilometer. To confirm the electropolymerization of conducting polymers, Raman spectra were recorded using a micro-Raman spectrometer (LabRAM ARAMIS, Horiba−Jobin−Yvon). Raman spectra acquired with notch filters cutting at 100 cm^{-1} using a Cobalt laser (473 nm, 5 mW at source) and a laser spot size of 1.5 μm.

Electrochemical Performance of Micro-Pseudocapacitor Devices. The electrochemical performance of the conducting polymer micro-pseudocapacitors were investigated in two electrode configuration in 1 M H_2SO_4. The gel electrolyte of poly(vinyl alcohol) (PVA)/H_2SO_4 was prepared as follows: 1 g of H_2SO_4 was added into 10 mL of deionized water, followed by 1 g of PVA powder. The whole mixture was heated to 85 °C, while stirring until the solution became clear. As the deposited polymer thickness is very small, gravimetric capacitance is not an appropriate parameter in evaluating the performance of these devices. Hence, we calculated the areal cell and volumetric capacitances of the micro-pseudocapacitors by taking the total area and volume of the electroactive electrodes into consideration. Cyclic voltammetry (CV) and galvanostatic charge−discharge (CD) measurements were performed using an electrochemical workstation (model 660D, CH Instruments, Austin, TX, USA). The CVs were tested in a voltage window between 0 and 0.8 V in a wide range of scan rates. The CDs were measured in the same voltage window under a wide range of current densities. The electrochemical impedance spectroscopy (EIS) data were measured using a Modulab (Solartron Analytical) electrochemical workstation in the frequency range from 100 kHz to 0.01 Hz at an open-circuit potential by applying a small sinusoidal potential of 10 mV signal. All measurements were performed at room temperature.

3. RESULTS AND DISCUSSION

The layout of conducting polymer micro-pseudocapacitor is schematically illustrated in Figure 1a. Microdevices with interdigitated electrode structure were fabricated employing conventional photolithography (see Supporting Information, Figure S1). Briefly, a 4 μm thick layer of photoresist was spun-coated over the glass substrate followed by UV exposure (dose, 200 mJ/cm^2) for 30 s. Next, the exposed regions of the

DOI: 10.1021/acsami.5b12784
ACS Appl. Mater. Interfaces 2016, 8, 12748−12755

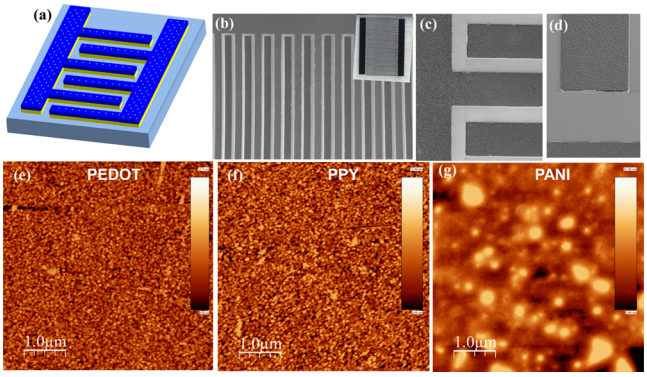

Figure 1. (a) Schematic representation of conducting polymer micro-pseudocapacitor. (b, c) SEM micrographs of PEDOT interdigitated fingers with an interspacing of 50 μm. (inset) Digital photograph of PEDOT MSC. (d) Tilt view of PEDOT thin film deposited over Au finger. (e–g) AFM topography images of PEDOT, PPY, and PANI thin films electrodeposited on Au surface.

photoresist were removed using a developer solution, with subsequent metal deposition (250 nm Au/20 nm Ti) by sputtering. At this stage, conducting polymer films (PEDOT, PPY, and PANI) were electropolymerized from their respective monomer electrolytic baths. Finally, lift-off using acetone with mild sonication resulted in the neat interdigitated fingers without having any material in the interspace regions as seen from the SEM micrographs in Figure 1b,c. Digital photograph in the inset shows full view of PEDOT microdevice. Conducting polymer thin films with a typical thickness of 100 nm were deposited through electrochemical deposition (see Raman data in Supporting Information, Figure S2). Electrochemical polymerization is preferred over the solution casting polymerization as the former offers good interfacial contact between the Au surface and the conducting polymer, avoiding possible interfacial impedance increase across the polymer/Au interface. The strong adherence of PEDOT film onto the Au surface is clearly evident, as it could sustain ultrasonication during the lift-off process. SEM tilt-view of a PEDOT/Au finger is shown in Figure 1d. AFM topography images of conducting polymer films are shown in Figure 1e–g, which show typical particulate morphology expected for a 100 nm thick film (see Supporting Information, Figure S2).

The frequency response of conducting polymer MPCs was investigated by electrochemical impedance spectroscopy. The impedance phase angles of PEDOT MPCs (thickness of ~100 nm) with interspacings of 100 (MPC 100), 50 (MPC 50), and 10 μm (MPC 10; shown in SEM micrographs in Figure S3) are plotted versus frequency and compared with commercial aluminum electrolytic capacitor (AEC) in Figure 2. Amazingly, the absolute phase angles of these devices are perfectly matching that of commerical AECs as shown in Figure 2a. It seems that the spacing between the fingers (in the range of 100–10 μm) has little influence on the frequency response characteristics of PEDOT MPCs as is evident from Figure 2a. Absolute phase angles of PEDOT MPCs are found to be very close to −90° at the low-frequency region (<60 Hz), exhibiting ideal capacitive response. However, for ac-line filtering applications, phase angle should be above −80° at 120 Hz. In our case, we found that PEDOT MSCs exhibited phase angles of −80.5° at 120 Hz, comparable to commercial AEC (phase angle of −84° at 120 Hz, as shown in Figure 2a). Usually,

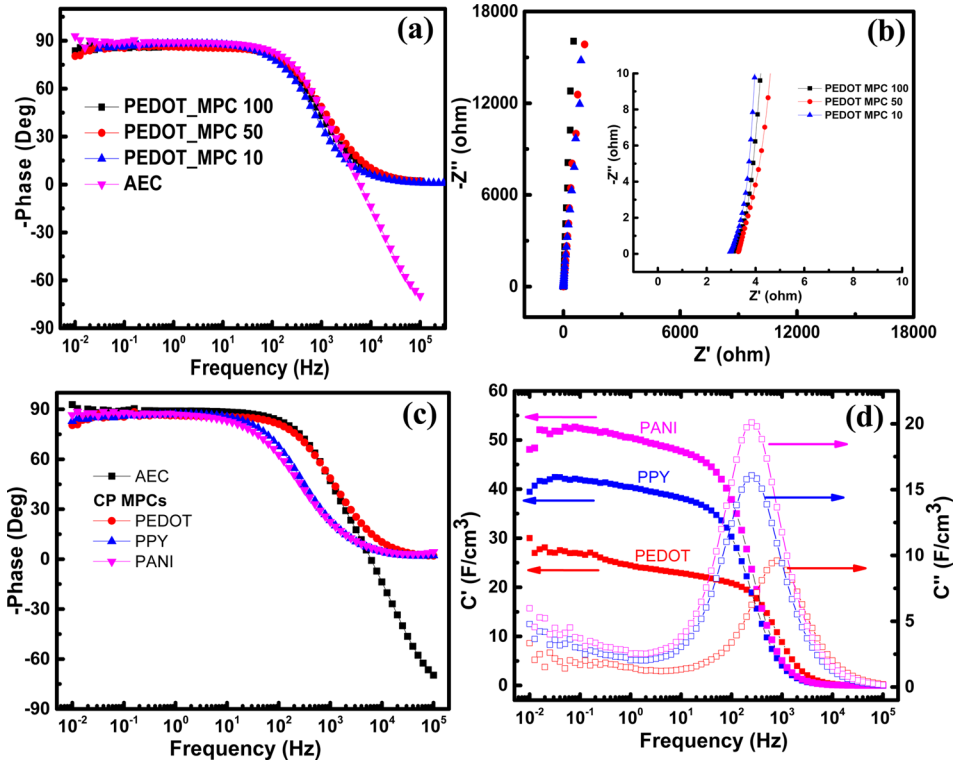

Figure 2. Frequency response characteristics of conducting polymer MPCs. (a) Bode phase angle plots of PEDOT MPCs (100, 50, 10 represent interspacings between the fingers) in comparison with commercial AEC (rated at 2 V), (b) Nyquist spectra over the entire frequency range. (inset) The high-frequency region of the spectra with nearly vertical nature. Comparison of (c) impedance phase angle and (d) C′ and C″ vs frequency of CP MPCs.

DOI: 10.1021/acsami.5b12784
ACS Appl. Mater. Interfaces 2016, 8, 12748–12755

crossover frequency at which the impedance phase angle reaches −45° is considered for comparison.[1,5] The typical crossover frequency (f) of PEDOT MPCs is found to be 1050 Hz. These crossover frequencies are comparable to that of 3D CNT/graphene[5] and graphene micro-electrochemical capacitors[1] reported in the literature. But the performance is far better than some forms of carbonaceous materials such as activated, onion-like carbon, and laser reduced graphene oxide micro-electrochemical capacitors.[23−26] This frequency response of PEDOT MPCs is comparable to that of ultrathin films of CNT[9] and reduced graphene oxide (rGO) reported in the literature.[11] The ac frequency response characteristics of PEDOT MPCs are comparable to that of electrical double-layer capacitors based on carbonaceous materials with varying thicknesses and configurations (see Tables S1 and S2, Supporting Information). This behavior indicates that PEDOT MPCs behave more like capacitor with faster ion diffusion kinetics. We believe that the optimal electronic and ionic resistances of PEDOT thin films are responsible for the excellent frequency response characteristics.[27] Further, we also investigated the frequency response of PEDOT MPC using solid-state electrolyte (PVA/H_2SO_4), which exhibit inferior frequency response compared to liquid electrolyte (see Figure S4 in the Supporting Information). Solid-state electrolyte shows lower ionic conductivity over liquid electrolytes due to reduction of ion mobility in the polymer matrix. Thus, solid-state electrochemical capacitors exhibit lower scan rate capabilities compared to their liquid counterparts. As shown in the Figure S4, solid-state device shows constant phase angle of −80.5° until 10 Hz unlike maintained until 120 Hz in the case of liquid electrolytes. Further, from the Nyquist spectra it is evident that solid-state device shows four times higher equivalent series resistance (ESR) compared to the device with liquid electrolyte. At present, commercial electrolytic capacitors also use liquid electrolytes that are being employed in ac-line filtering applications. The challenging aspect lies in developing solid-state electrolytes with similar ionic conductivity as that of liquid media that can help in terms of safety and encapsulation while offering the specific capabilities such as ac-line filtering. Further, the stability of PEDOT MPCs was tested by continuously doing charge/discharge between 0 to 0.8 V at a current density of 0.15 mA/cm^2, as shown in Figure S5. Clearly, PEDOT MPCs show capacitance retention of 90% and Coulombic efficiency of nearly 100% over 10 000 cycles.

Porosity, intrinsic electrical conductivity, and redox behavior of the electrode material are the major governing factors that determine the frequency response of an electrochemical capacitor besides the electrode architecture.[2,7] As shown in Figure 2b, Nyquist plots shown for PEDOT MPCs are seen parallel to $-Z''$ axis with the absence of semicircle in the high-frequency region, which implies that excellent ohmic coupling between the Au current collector and PEDOT polymeric layers. Information about the behavior of the electrode materials can be estimated from the line intersecting the real axis at an angle of 45° in a Nyquist plot.[1] PEDOT MPC exhibits little or negligible porosity effect as is evident from high-frequency region, shown in Figure 2b (also see the inset).

Impedance phase angles of other conducting polymer MPCs such as PPY and PANI were studied and compared with PEDOT, as shown in Figure 2c. It can be seen that PPY and PANI MSCs exhibit phase angles of 60−65° at a frequency of 120 Hz, while the crossover frequencies are in the range of 250−300 Hz. Certainly, these conducting polymer MSCs (PPY and PANI) exhibit inferior ac-response characteristics compared to PEDOT, which is attributed to the electronic conductivity and intrinsic redox nature of the electrodes.[15] Typical conductivities of PEDOT, PPY, and PANI thin films were found to be 108, 9.2, and 2.9 S/cm, respectively (see Supporting Information, Figure S6).[15] The diminished frequency response of PPY and PANI MPCs can be attributed to the greater redox activity (extent of doping level is more for PANI and PPY compared to PEDOT) and lower conductivity compared to PEDOT. The reason for the absence of a clear semicircle for PPY and PANI MPCs could be due to the thin-film morphology and the in-plane configuration of electrodes while having the ohmic coupling between the current collectors and conducting polymeric layers (see Supporting Information, Figures S7−S11). Thus, PEDOT MPC behaves more like a capacitor, while PPY and PANI MPCs may exhibit charge leakage due to Faradaic charge transfer.[2,28]

The real (C') and imaginary (C'') parts of capacitances are extracted from the electrochemical impedance data of conducting polymer MPCs. Figure 2d displays plot of C' and C'' versus frequency (calculated using the equations mentioned in the Supporting Information). Notice that C' of PEDOT MPC remains unchanged up to 120 Hz, suggesting excellent capacitive behavior compared to PPY and PANI MPCs. It is interesting to compare the characteristic relaxation time constant ($\tau_0 = 1/f_0$), which is the time required for discharging a capacitor with an efficiency greater than 50%.[16] This can be obtained from the frequency (f_o) at which the imaginary capacitance C'' becomes maximum. The relaxation time constant is found to be 1 ms for PEDOT MPCs and 3−4 ms for the PPY and PANI MPCs. However, PPY and PANI MPCs exhibit a volumetric capacitance of 40−50 F/cm^3, superior to PEDOT MPC (30 F/cm^3). PEDOT, due to high monomer mass and low doping level, exhibits lower capacity in comparison to PPY and PANI.[29] Thus, PPY and PANI, due to their intrinsic redox characteristics, can contribute to the higher capacity values, while the intrinsic conducting nature of PEDOT is responsible for its excellent ac-response characteristics.[15] The resistor−capacitor (RC) time constant (τ_{RC}) at 120 Hz is found to be 0.21 ms for PEDOT MPCs. This value is much shorter than 8.3 ms period required for 120 Hz filtering, matching that of commercial AEC (0.15 ms). Carbon-based electrochemical capacitors with internal porosity will have distributed charge storage, exhibiting multiple time constants associated with the RC networks corresponding to the dispersed porous structure.[1] Consequently, quoting of single RC time constant for such a device may not be appropriate; a better concept would be to use "characteristic response time", which is related to the energy extraction rate. On the basis of this concept, the typical activated carbon type EDLC will have a characteristic response time of ∼1 s. However, the characteristic response time should be 8.3 ms (to respond capacitively at 120 Hz) for ac-line filtering applications. Thus, activated carbon EDLC is incapable of responding at 120 Hz. (It behaves like a resistor rather than a capacitor at 120 Hz. as the characteristic response time of 1 s is far higher than 8.3 ms.) It is evident from the impedance data shown in Figure 2a; PEDOT MPCs clearly can respond capacitively at 120 Hz and can be represented by an equivalent series-RC circuit model (with a single time constant of 0.21 ms).

The excellent frequency response of PEDOT MPCs can be attributed to the thin-film nature of conducting PEDOT with proper interfacial characteristics as well as the in-plane

DOI: 10.1021/acsami.5b12784
ACS Appl. Mater. Interfaces 2016, 8, 12748−12755

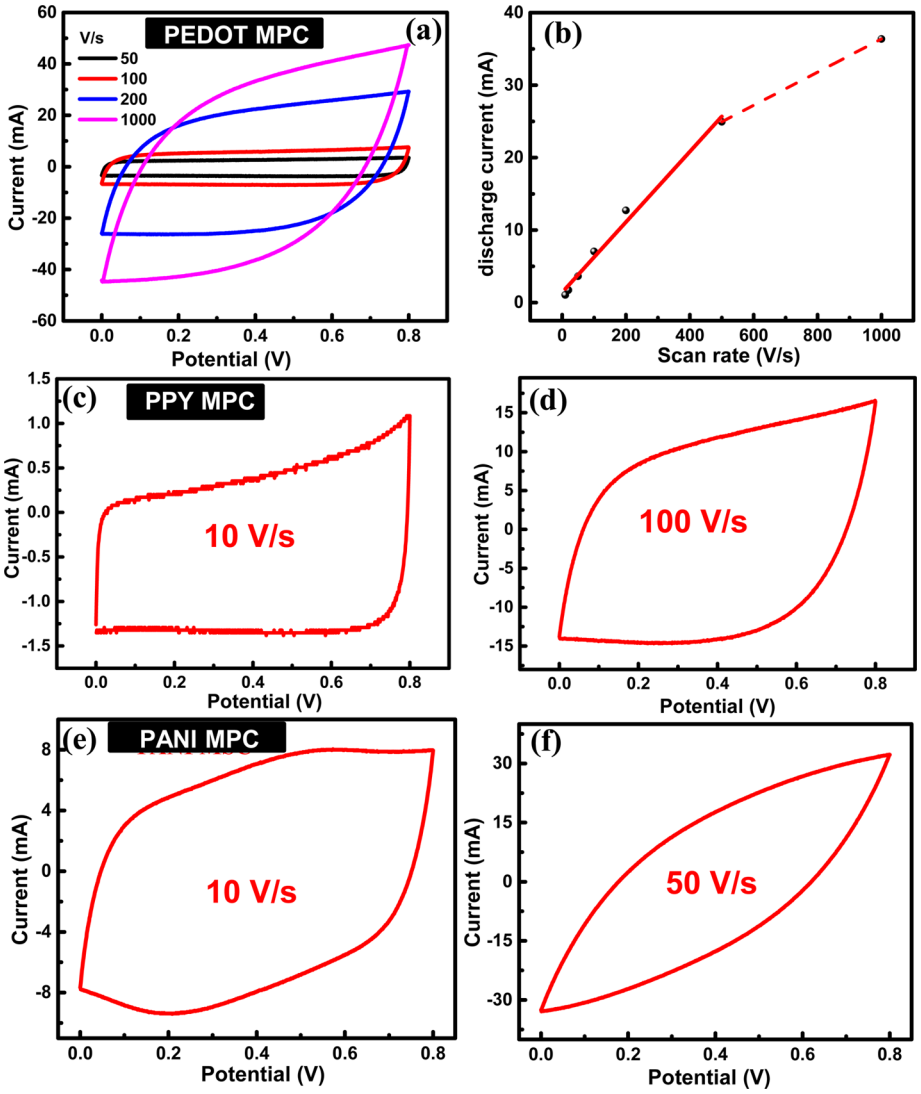

Figure 3. Electrochemical performance of conducting polymer MPCs. (a) CVs and (b) variation of discharge current with scan rate of PEDOT MPC. CVs of PPY (c) and (d) PANI MPCs (e, f).

configuration of electrode architecture; these two factors together contribute to the lower values of electronic and ionic resistances. Recently, there have been siginificant amounts of research papers focusing on the frequency response characteristics of open porous carbon forms such as graphene and CNTs in various electrode architectures. Pseudocapacitors such as conducting polymers may involve Faradaic charge storage besides the coupling of double-layer formation, but the electrical response is similar to that of shown by a capacitor. At 120 Hz, PEDOT MPC has a volumetric capacitance of 19 F/cm^3 with an ESR of 5.8 Ω and corresponding time constant of 209 μs. The capacitance density is found to be 12 FV/cm^3 (for active layer thickness only) and 3 FV/cm^3 (considering thickness of both current collectors and active material; aqueous electrolyte, voltage window of 0.8 V), which is far superior to the low-voltage (2 V, areal capacitance of 40 μF/cm^2) aluminum anode foil (KDK, Tokyo, Japan) with capacitance density values up to ∼0.14 FV/cm^3.[1] Typically, AECs rated at 2 V or higher are being employed in ac-line filtering of portable electronic devices. Thus, PEDOT MPCs exhibit superior capacitance density by at least an order of magnitude over commercial AECs, while matching the frequency response characteristics.

As shown in Figure 3a, CVs of PEDOT MPCs are quite rectangular in nature until ultra high scan rates of 1000 V/s, indicating the capacitive nature of PEDOT MPCs. Discharge current values are plotted versus scan rate and show linear behavior up to the scan rate of 500 V/s, beyond which a slight deviation from linearity is observed (see Figure 3b). Since the entire volume of the thin film can be accessed by the electrolyte ions without any diffusion limitations, ultrahigh scan rate capability is observed for PEDOT MPCs. However, in the case of PPY MPCs, as shown in Figure 3c,d, rectangle CV shape is retained only up to 100 V/s. Similarly, PANI MPC shows broad redox peaks at a scan rate of 10 V/s, indicating its Faradaic nature of charge storage (see Figure 3e). Further, at a high scan rate of 50 V/s, PANI MPCs exhibit complete deviation from the rectangular CV shape, indicating the dominating resistive nature of PANI MPCs at higher scan rates (see Figure 3f). Thus, the intrinsic redox behavior of PANI contributes to the higher values of capacitance at moderate scan rates (up to 10 V/s) but loses its pseudocapacitive nature at higher scan rates (>50 V/s). This

DOI: 10.1021/acsami.5b12784
ACS Appl. Mater. Interfaces 2016, 8, 12748−12755

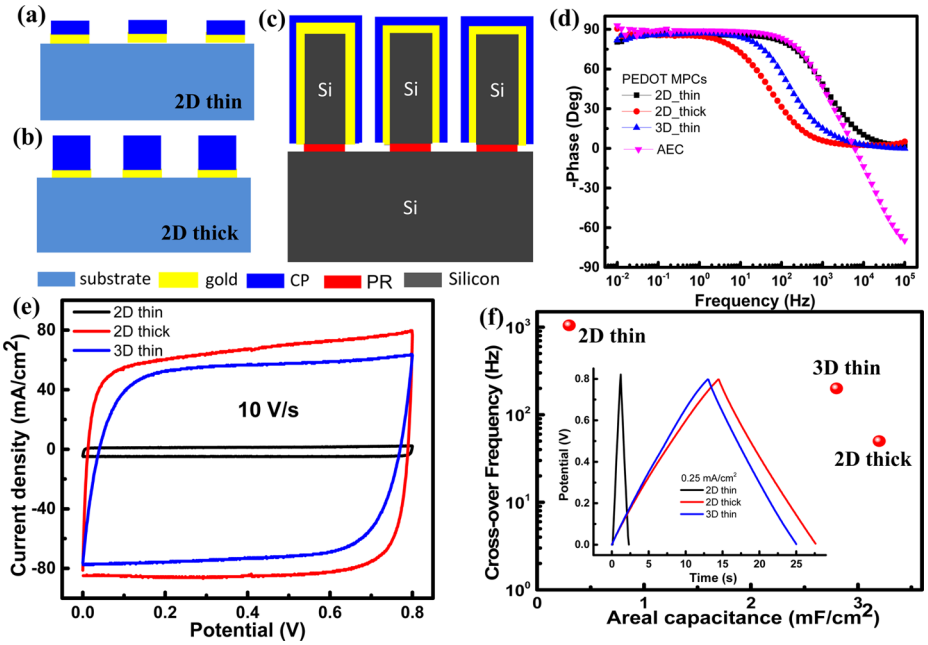

Figure 4. Schematic of PEDOT MPCs with (a) 2D thin, (b) 2D thick, and (c) 3D thin-film electrodes. (d) Comparison of Bode phase plots of PEDOT MPCs in 2D and 3D architectures. (e) CVs of PEDOT MPCs in 2D and 3D formats. (f) Crossover frequency (corresponding phase angle of −45°) vs areal capacitance of various PEDOT MPCs. (inset) The comparison of CDs of 2D thin and thick, 3D thin PEDOT MPCs.

result implies that charge leakage by Faradaic charge transfer could limit the kinetics of a pseudocapacitor device.[2,30]

Despite the fact that PEDOT MPCs with thin polymer films (see schematic in Figure 4a) exhibit good ac response, they have limited areal capacitance (0.3 mF/cm^2 for 100 nm thin film). To increase the capacitance, we attempted two different approaches. In one case, as shown in the schematic of Figure 4b, thicker PEDOT films (thickness, 1 μm) were deposited by increasing electrodeposition time. In another case, 3D interdigitated Si fingers (thickness >300 μm) were fabricated by employing micro-electromechanical systems technologies to increase loading of active materials in a given footprint area.[16,17] PEDOT thin films were deposited on metallized 3D Si fingers (as described in the Experimental Section; see also Figure S12, Supporting Information) and shown in Figure 4c. Bode phase angle plots of PEDOT MPCs in these various electrode architectures are compared with the commercial AEC as shown in Figure 4d. As was discussed earlier, 2D thin-film PEDOT MPCs exhibit good frequency response characteristics and indeed match the electrochemical performance of commercial AEC. Thicker PEDOT MPCs (thickness, 1 μm) in the 2D design exhibit a phase angle of −35° at 120 Hz with a crossover frequency (corresponding phase angle of −45°) of 50 Hz (see red curve in Figure 4d). Similarly, as shown in Figure S10a, the crossover frequency of PPY MPCs at −45° diminished from 425 to 37 Hz when the thickness was increased from 100 to 500. Similarly, for PANI MPCs (shown in Figure S11a), crossover frequency at −45° was observed to be 265, 32, and 2.3 Hz for 100, 300, and 500 nm films, respectively. The inferior frequency response characteristics of 2D thick PEDOT MPCs can be attributed to the longer ion diffusion lengths and increased electrical resistivity of the thicker films. Similar observations were made in the case of RuO_2 pseudocapacitors.[2]

Interestingly, the 3D PEDOT MPCs exhibit a phase angle of −60° at 120 Hz with a crossover frequency of 200 Hz, much better than 2D thick PEDOT MPCs (see blue curve in Figure 4d). It was observed that 2D thick and 3D thin PEDOT MPCs exhibit an enhanced areal capacitance up to 10 times higher than 2D thin-film PEDOT MPCs. This is due to maximum loading of electroactive materials in a given footprint area. As shown in Figure 4e, CVs of PEDOT MPCs are seen to be quite rectangular, behaving like a capacitor irrespective of the design. Areal capacitance of both 2D thick and 3D thin PEDOT MPCs are found to be ∼3 mF/cm^2 (0.3 mF/cm^2 for 2D thin film) at a current density of 0.25 mA/cm^2 (see the inset of Figure 4f). As shown in Figure 4f, 2D thin-film PEDOT MPCs exhibit excellent frequency response but suffer from lower areal capacitance, while 2D thick PEDOT MPCs exhibit poor frequency response with higher areal capacitance. Thus, the tradeoff between the capacitance and frequency response can be optimized by considering the 3D architecture. Clearly, the 3D PEDOT MPCs exhibit similar areal capacitance with superior frequency response compared to 2D thick PEDOT MPCs (see Figure 4e). In other words, 3D PEDOT architecture seems to maintain similar areal capacitance to 2D thick PEDOT MSCs but with better frequency response. Thus, our results clearly indicate that 3D architecture is a good choice for fabricating micro-electrochemical capacitors that can maintain excellent areal capacitance and frequency response.

4. CONCLUSIONS

In summary, we have studied the frequency response of micro-pseudocapacitors based on conducting polymer electrodes such as PEDOT, PPY, and PANI, fabricated in both 2D and 3D architectures. Among the polymeric materials studied, PEDOT micro-pseudocapacitors exhibit phase angle of −80.5° at 120 Hz, comparable to that of commercial bulky electrolytic capacitors but with an order of magnitude higher capacitance density. This can be attributed to the higher electrical conductivity and fast surface redox reactions of PEDOT over other conducting polymers. Moreover, the existence of tradeoff between areal capacitance (C_A) and frequency response in the

DOI: 10.1021/acsami.5b12784
ACS Appl. Mater. Interfaces 2016, 8, 12748−12755

2D configuration was optimized to some extent by choosing 3D architecture. Our work clearly demonstrated that properly designed micro-pseudocapacitors can exhibit frequency response matching that of commercial electrolytic capacitors. Further, this study may open new avenues in exploring the 3D micro-electrochemical capacitors composed of pseudocapacitive materials to maintain the optimal balance between areal capacitance and frequency response.

■ ASSOCIATED CONTENT

Supporting Information

The Supporting Information is available free of charge on the ACS Publications website at DOI: 10.1021/acsami.5b12784.

Schematic illustration of fabrication of conducting polymer micro-pseudocapacitors (MPCs). SEM micrographs of electrodeposited PEDOT, PPY, and PANI thin films. Raman spectra of electrodeposited CPs. SEM micrographs of PEDOT MPCs with interspacing of 10, 50, and 100 μm, finger width of 100 μm is same throughout. Comparison of Bode phase angle versus frequency and Nyquist spectra of PEDOT MPCs with aqueous (black curve) and solid-state (red curve) electrolytes. Cycling stability and Coulombic efficiency of PEDOT MPC over 10 000 cycles at a current density of 0.15 mA/cm^2 in 1 M H_2SO_4; inset shows the frequency response before and after cycling. Four probe current−voltage characteristics of conducting polymer thin films. Typical conductivities of PEDOT, PPY, and PANI thin films (thickness of 100 nm) are found to be 108, 9.2, and 2.9 S/cm, respectively. Nyquist spectra of PEDOT, PPY, and PANI MPCs; inset shows the high-frequency region of the spectra. Comparison of Nyquist spectra of conducting polymer micro-electrochemical capacitors with AEC. Equivalent circuit model for fitting the impedance data of conducting polymer micro-supercapacitors. Nyquist plots and fitted plot for PEDOT, PPY, PANI. Percentage contribution of double-layer and pseudocapacitive contributions for the conducting polymer micro-supercapacitors, obtained after fitting the impedance data to an equivalent circuit. Bode phase angle plots and CVs of PPY MPCs with different thicknesses. Bode phase angle plots and CVs of PANI MPCs with different thicknesses. Schematic illustration of Si etch-through process employing photolithography and DRIE. Inset shows micrograph of interdigitated 3D Si wall structures. Electrochemical performance comparison of carbonaceous materials comparison of the electrochemical performance of the micro-electrochemical capacitors reported in the literature. Electrochemical performance of conducting polymer micro-pseudocapacitors in this work. (PDF)

■ AUTHOR INFORMATION

Corresponding Author

*E-mail: husam.alshareef@kaust.edu.sa.

Author Contributions

[+]These authors contributed equally to the work.

Notes

The authors declare no competing financial interest.

■ ACKNOWLEDGMENTS

Research reported in this publication was supported by King Abdullah University of Science and Technology (KAUST). Authors thank the Advanced Nanofabrication, Imaging and Characterization Laboratory at KAUST for their excellent support.

■ REFERENCES

(1) Miller, J. R.; Outlaw, R.; Holloway, B. Graphene Double-Layer Capacitor with AC Line-Filtering Performance. *Science* **2010**, *329*, 1637−1639.

(2) Conway, B. E. *Electrochemical Supercapacitors: Scientific Fundamentals and Technological Applications;* Plenum Press, Springer: New York, 1999.

(3) Miller, J. R.; Burke, A. F. Electrochemical Capacitors: Challenges and Opportunities for Real-World Applications. *Electrochem. Soc. Interface.* **2008**, *17*, 53−57.

(4) De Levie, R.; Delahay, P. Electrochemical Response of Porous and Rough Electrodes. *Advances in electrochemistry and electrochemical engineering* **1967**, *6*, 329−397.

(5) Lin, J.; Zhang, C.; Yan, Z.; Zhu, Y.; Peng, Z.; Hauge, R. H.; Natelson, D.; Tour, J. M. 3-Dimensional Graphene Carbon Nanotube Carpet-based Microsupercapacitors with High Electrochemical Performance. *Nano Lett.* **2013**, *13*, 72−78.

(6) Sheng, K.; Sun, Y.; Li, C.; Yuan, W.; Shi, G. Ultrahigh-Rate Supercapacitors based on Eletrochemically Reduced Graphene Oxide for Ac Line-Filtering. *Sci. Rep.* **2012**, *2*, 247−251.

(7) Boos, D.; Argade, S. In *Historical Background and New Perspectives for Double-Layer Capacitors,* 1st International Seminar on Double-Layer Capacitors and Similar Energy Storage Devices, Deerfield Beach, FL, 1991.

(8) Rangom, Y.; Tang, X.; Nazar, L. F. Carbon Nanotube-based Supercapacitors with Excellent AC Line Filtering and Rate Capability via Improved Interfacial Impedance. *ACS Nano* **2015**, *9*, 7248−7255.

(9) Yoo, Y.; Kim, S.; Kim, B.; Kim, W. 2.5 V Compact Supercapacitors based on Ultrathin Carbon Nanotube Films for AC Line Filtering. *J. Mater. Chem. A* **2015**, *3*, 11801−11806.

(10) Laszczyk, K. U.; Kobashi, K.; Sakurai, S.; Sekiguchi, A.; Futaba, D. N.; Yamada, T.; Hata, K. Microsupercapacitors: Lithographically Integrated Microsupercapacitors for Compact, High Performance, and Designable Energy Circuits. *Adv. Energy Mater.* **2015**, *5*, 1500741.

(11) Wu, Z. S.; Liu, Z.; Parvez, K.; Feng, X.; Müllen, K. Ultrathin Printable Graphene Supercapacitors with AC Line-Filtering Performance. *Adv. Mater.* **2015**, *27*, 3669−3675.

(12) Yoo, Y.; Kim, M.-S.; Kim, J.-K.; Kim, Y. S.; Kim, W. Fast-Response Supercapacitors with Graphitic Ordered Mesoporous Carbons and Carbon Nanotubes for AC Line Filtering. *J. Mater. Chem. A* **2016**, *4*, 5062−5068.

(13) Lim, J.; Maiti, U. N.; Kim, N. Y.; Narayan, R.; Lee, W. J.; Choi, D. S.; Oh, Y.; Lee, J. M.; Lee, G. Y.; Kang, S. H.; Kim, H.; Kim, Y. H.; Kim, S. O. Dopant-Specific Unzipping of Carbon Nanotubes for Intact Crystalline Graphene Nanostructures. *Nat. Commun.* **2016**, *7*, 10364.

(14) Beidaghi, M.; Gogotsi, Y. Capacitive Energy Storage in Micro-Scale Devices: Recent Advances in Design and Fabrication of Micro-Supercapacitors. *Energy Environ. Sci.* **2014**, *7*, 867−884.

(15) Snook, G. A.; Kao, P.; Best, A. S. Conducting Polymer based Supercapacitor Devices and Electrodes. *J. Power Sources* **2011**, *196*, 1−12.

(16) Sun, W.; Zheng, R.; Chen, X. Symmetric Redox Supercapacitor Based on Micro-Fabrication with Three-Dimensional Polypyrrole Electrodes. *J. Power Sources* **2010**, *195*, 7120−7125.

(17) Shen, C.; Wang, X.; Li, S.; Zhang, W.; Kang, F. A High Energy Density Micro Supercapacitor of Asymmetric MnO_2 Carbon Configuration by using Micro Fabrication Technologies. *J. Power Sources* **2013**, *234*, 302−309.

(18) Wang, K.; Wu, H.; Meng, Y.; Wei, Z. Conducting Polymer Nanowire Arrays for High Performance Supercapacitors. *Small* **2014**, *10*, 14−31.

DOI: 10.1021/acsami.5b12784
ACS Appl. Mater. Interfaces 2016, 8, 12748−12755

(19) Wang, K.; Zou, W.; Quan, B.; Yu, A.; Wu, H.; Jiang, P.; Wei, Z. An All-Solid-State Flexible Micro-supercapacitor on a Chip. *Adv. Energy Mater.* **2011**, *1*, 1068−1072.
(20) Patra, S.; Munichandraiah, N. Supercapacitor Studies of Electrochemically Deposited PEDOT on Stainless Steel Substrate. *J. Appl. Polym. Sci.* **2007**, *106*, 1160−1171.
(21) Kurra, N.; Jiang, Q.; Alshareef, H. N. A General Strategy for the Fabrication of High Performance Microsupercapacitors. *Nano Energy* **2015**, *16*, 1−9.
(22) Horcas, I.; Fernández, R.; Gomez-Rodriguez, J.; Colchero, J.; Gómez-Herrero, J.; Baro, A. WSXM: A Software for Scanning Probe Microscopy and A Tool for Nanotechnology. *Rev. Sci. Instrum.* **2007**, *78*, 013705.
(23) Pech, D.; Brunet, M.; Taberna, P.-L.; Simon, P.; Fabre, N.; Mesnilgrente, F.; Conédéra, V.; Durou, H. Elaboration of a Microstructured Inkjet-Printed Carbon Electrochemical Capacitor. *J. Power Sources* **2010**, *195*, 1266−1269.
(24) Pech, D.; Brunet, M.; Durou, H.; Huang, P.; Mochalin, V.; Gogotsi, Y.; Taberna, P.-L.; Simon, P. Ultrahigh Power Micrometre Sized Supercapacitors Based on Onion-Like Carbon. *Nat. Nanotechnol.* **2010**, *5*, 651−654.
(25) Gao, W.; Singh, N.; Song, L.; Liu, Z.; Reddy, A. L. M.; Ci, L.; Vajtai, R.; Zhang, Q.; Wei, B.; Ajayan, P. M. Direct Laser Writing of Micro-Supercapacitors on Hydrated Graphite Oxide Films. *Nat. Nanotechnol.* **2011**, *6*, 496−500.
(26) El-Kady, M. F.; Kaner, R. B. Scalable Fabrication of High-Power Graphene Micro-Supercapacitors for Flexible and On-Chip Energy Storage. *Nat. Commun.* **2013**, *4*, 1475.
(27) Kurra, N.; Hota, M.; Alshareef, H. N. Conducting Polymer Micro-Supercapacitors for Flexible Rnergy Storage and AC Line-Filtering. *Nano Energy* **2015**, *13*, 500−508.
(28) Taberna, P.; Simon, P.; Fauvarque, J.-F. Electrochemical Characteristics and Impedance Spectroscopy Studies of Carbon-Carbon Supercapacitors. *J. Electrochem. Soc.* **2003**, *150*, A292−A300.
(29) Snook, G. A.; Chen, G. Z. The Measurement of Specific Capacitances of Conducting Polymers using the Quartz Crystal Microbalance. *J. Electroanal. Chem.* **2008**, *612*, 140−146.
(30) Talbi, H.; Just, P.-E.; Dao, L. Electropolymerization of Aniline on Carbonized Polyacrylonitrile Aerogel Electrodes: Applications for Supercapacitors. *J. Appl. Electrochem.* **2003**, *33*, 465−473.

DOI: 10.1021/acsami.5b12784
ACS Appl. Mater. Interfaces 2016, 8, 12748−12755